NeuroImage 321 (2025) 121511

Contents lists available at ScienceDirect

NeuroImage

journal homepage: www.elsevier.com/locate/ynimg

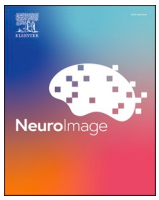

Comparative evaluation of single- and multi-delay arterial spin labeling MRI in preterm neonates

Yeva Prysiazhniuk [a,b], Sasha Alexander [c], Rui Duarte Armindo [d], Elizabeth Tong [e], Kristen W Yeom [c], Jakub Otáhal [a], Martin Kynčl [b], Michael Moseley [e], Jan Petr [f,g,1], Moss Y Zhao [c,1], Gary K Steinberg [c,1,*]

[a] Department of Pathophysiology, Second Faculty of Medicine, Charles University, Prague, Czech Republic
[b] Department of Radiology, Second Faculty of Medicine, Charles University and University Hospital Motol, Prague, Czech Republic
[c] Department of Neurosurgery, Stanford University, Stanford, CA, United States
[d] Department of Neuroradiology, Western Lisbon Local Health Unit, Lisbon, Portugal
[e] Department of Radiology, Stanford University, Stanford, CA, United States
[f] Helmholtz-Zentrum Dresden-Rossendorf, Institute of Radiopharmaceutical Cancer Research, Dresden, Germany
[g] Department of Radiology and Nuclear Medicine, Amsterdam Neuroscience, Amsterdam University Medical Center (Location VUmc), Amsterdam, Netherlands

ARTICLE INFO

Keywords:
ASL
perfusion MRI
preterm neonates
cerebral blood flow
arterial transit time

ABSTRACT

Introduction: Preterm neonates are vulnerable to brain injuries from disrupted cerebral blood flow (CBF). Achieving high-quality MRI remains a major challenge in neonatal neuroimaging. Arterial Spin Labeling (ASL) MRI offers non-invasive, quantitative CBF assessment, but is understudied in neonates. This study evaluates the feasibility of ASL in non-sedated preterm neonates.

Methods: Preterm neonates (n=48, 25 male, post-natal age 9.74±4.96 weeks, gestational age 28.74±2.6 weeks) underwent T1-weighted (T1w), T2-weighted (T2w), and single- and multi-delay (3 and 7 delays) ASL scans. Image quality was rated as "good", "acceptable", or "unusable" and compared across modalities. Cortical CBF and arterial transit time (ATT) were quantified and analyzed using paired t-tests and Cohen's d. Associations with sex and age were assessed using correlation and regression models.

Results: Multi-delay ASL demonstrated the highest rate of acceptable images (<10% "unusable"), T2w scans outperformed T1w in quality (4.2% vs. 25% "unusable", $p<0.01$). Single-delay ASL yielded significantly lower cortical CBF compared to multi-delay ASL ($p<0.001$, $d\geq1.12$), with sex differences observed: single-delay CBF was lower in females ($p=0.035$, $d=0.72$), and ATT was longer in males ($p=0.045$, $d=0.60$). CBF positively correlated with postmenstrual and postnatal age, especially for three-delay ASL.

Conclusions: Multi-delay ASL is the favorable technique for neonatal neuroimaging based on image quality and hemodynamic measurements. Sex- and age-related hemodynamic variations underscore the importance of techniques distinguishing ATT and CBF components for improved neonatal perfusion neuroimaging. Despite frequent motion artifacts, ASL quality was comparable to structural scans. These findings support broader clinical adoption of multi-delay ASL in neonatal imaging protocols.

1. Introduction

Preterm birth, defined as delivery before 37 completed weeks of gestation, is the leading cause of neonatal mortality and morbidity worldwide (Ohuma et al., 2023). Survivors of preterm birth frequently experience long-term neurodevelopmental impairments, including cognitive and motor deficits. A key physiological hallmark for these impairments is the reduced cerebral blood flow (CBF), which has been strongly correlated with severe brain injuries such as intraventricular hemorrhage (IVH) and periventricular leukomalacia (PVL) (Hak et al., 2022, Fukuda et al., 2008, Langley et al., 2022), as well as the long-term risks of neurodevelopmental impairments (Davis et al., 2014, Sarda et al., 2021). Notably, preterm neonates demonstrate distinct CBF patterns compared to their full-term counterparts (Bouyssi-Kobar et al.,

* Corresponding author.
E-mail address: cerebral@stanford.edu (G.K. Steinberg).
[1] Co-Senior Authors.

https://doi.org/10.1016/j.neuroimage.2025.121511
Received 14 May 2025; Received in revised form 22 September 2025; Accepted 6 October 2025
Available online 9 October 2025

2018), particularly during the first postnatal weeks. This highlights the need for robust, non-invasive techniques capable of accurately monitoring cerebral perfusion during early neonatal care.

Several imaging and monitoring modalities have been used to assess cerebral hemodynamics in neonates. Near-infrared spectroscopy (NIRS) is commonly employed for assessing cerebral perfusion and autoregulation in preterm infants, but its indirect CBF measurement, lack of clinical consensus on its routine use, and inter-vendor variability limit its reliability (Singh et al., 2020, Kleiser et al., 2016). Doppler ultrasound, while accessible, is constrained by its location dependence and inability to provide direct or regional CBF measurement (Zamora et al., 2014). Xenon-133 and 15O-water PET, though historically significant and important for validating results, are invasive and unsuitable for routine use in newborns (Andersen et al., 2019, Younkin et al., 1988, Younkin et al., 1987). These limitations have motivated increasing interest in MRI-based approaches, however, obtaining high-quality MR images in neonates remains challenging (Hu et al., 2025).

Arterial spin labeling (ASL) MRI enables non-invasive absolute quantification of regional CBF. Specifically, ASL has proven effective in assessing the hemodynamic status of preterm infants, distinguishing between degrees of prematurity and associated brain perfusion abnormalities (Bouyssi-Kobar et al., 2018, Dubois et al., 2021, Tuura et al., 2024, Zun et al., 2021). Single-delay ASL, though the most common option, can misestimate CBF in cases of delayed blood arrival, which is common in this population. Multi-delay ASL techniques, particularly Hadamard-encoded protocols, enable estimation of both CBF and ATT by sampling a broader range of post-labeling delays (PLDs), potentially offering more robust quantification (Woods et al., 2024). However, ASL is fundamentally a subtraction method, making it particularly sensitive to motion artifacts — a significant concern for neonatal imaging where sedation is typically avoided. Despite growing interest in applying ASL in neonatal neuroimaging, several critical knowledge gaps remain: the comparative performance, image quality, and physiological sensitivity of single- versus multi-delay ASL have not been fully elucidated; the feasibility of ASL in non-sedated preterm neonates has not been systematically investigated; and it remains unclear how ASL data quality in this population compares to conventional structural scans. Furthermore, CBF correlations with clinical factors including postmenstrual age (PMA), gestational age (GA), postnatal age (PNA), and birth weight, sex, and etiology of premature birth have not been comprehensively evaluated or compared between single- and multi-delay ASL acquisition methods in this vulnerable population.

In this study, we evaluate hemodynamic measurements in 48 non-sedated preterm neonates using single- and multi-delay ASL techniques. We assess and compare the quality of ASL data alongside T1-weighted (T1w) and T2-weighted (T2w) structural scans. Our analysis compares cortical gray matter CBF measurements of single- and multi-delay ASL methods acquired within a single session, investigates arterial transit time (ATT) as a confounder in CBF quantification, and explores correlations with clinical parameters, such as sex, cause of premature birth, PMA, GA, and PNA. Additionally, we examine hemispheric asymmetry and how fetal-type posterior cerebral artery variants influence CBF patterns.

2. Methods

2.1. Participant information

This study included subjects scanned at Lucile Packard Children's Hospital Stanford between August 2022 and December 2023. All participants were scanned using a standardized clinical protocol for preterm neonates that incorporated structural and perfusion MRI sequences. Inclusion criteria were: (1) gestational age at birth <37 weeks, (2) successful completion of the ASL protocol, and (3) absence of major structural abnormalities on diagnostic MRI evaluated by board-certified pediatric neuroradiologists (KWY and ET). Due to scanner upgrades or protocol changes during the study period, some neonates did not undergo the complete ASL protocol. However, these variations did not introduce any systematic bias. A total of 48 neonates met all inclusion criteria and were analyzed. Ethics approval was granted by Stanford IRB's Administrative Panel on Human Subjects in Medical Research, and informed parental consent for secondary use of the data was obtained in accordance with the Declaration of Helsinki.

2.2. Clinical information

Clinical records were reviewed to determine the cause of preterm labor, which was classified into the following categories: spontaneous labor with intact membranes, preterm premature rupture of membranes (PPROM), labor induction or cesarean delivery due to maternal indications, and labor induction or cesarean delivery due to fetal indications (Goldenberg et al., 2008).

2.3. MRI acquisition

MRI data acquisition was conducted on a 3T GE Premier (GE Healthcare, Waukesha, USA) with a 48-channel head coil. The "feed and bundle" method was employed for imaging without the use of sedation in all participants. All included participants underwent T1-weighted (3D FSPGR, TR/TE 6.3/2.5 ms, flip angle 12°, voxel size isotropic 1 mm^3) and T2-weighted (2D FSE, TR/TE 2700/110.5 ms, flip angle 111°, voxel size 0.5 × 0.5 × 2.5 mm^3) scans.

Three types of background-suppressed pseudo-continuous ASL (PCASL) with M0 were acquired:

- single-delay - $PCASL_{1PLD}$ (post-labeling delay (PLD) 1525 ms; labeling duration (LD) 1450 ms; acquisition duration 4 min 15 s);
- Hadamard-encoded three-delay - $PCASL_{3PLD}$ (PLD 700, 2000, and 3300 ms; LD 1300 ms; acquisition duration 4 min 50 s);
- Hadamard-encoded seven-delay - $PCASL_{7PLD}$ (PLD 700, 1250, 1800, 2350, 2900, 3450, and 4000 ms; LD 550 ms; acquisition duration 4 min 20 s).

Further details of the MRI acquisition protocol are provided in Supplementary Table S1.

2.4. Image analysis

T1w, T2w, raw ASL files, and scanner-reconstructed CBF (CBF_{1PLD}, and arterial-time corrected CBF_{3PLD} and CBF_{7PLD}) and ATT (ATT_{3PLD} and ATT_{7PLD}) were exported from the scanner. Cases with missing raw ASL files were excluded from the analysis (n=2). Brain segmentation in the native space was performed using the BIBSnet (Baby and Infant Brain Segmentation Neural Network) pipeline (Hendrickson et al., 2025). Maps of total gray matter (GM), white matter (WM), and cortical GM (excluding the deep GM regions) were extracted from the resulting segmentations. CBF maps were registered to T1w scans in the native space using affine transformation as a part of the standard processing pipeline. Effective resolution of ASL scans was estimated to be able to account for through-slice blurring as well as different FOV of the sequences, using the implementation available in the ExploreASL pipeline (Mutsaerts et al., 2020). A Gaussian point spread function (PSF) was

assumed and its full-width at half maximum was estimated iteratively by minimizing the root mean square difference between the CBF maps and pseudo-CBF image. In the first step, GM and WM masks were used to calculate partial-volume corrected GM and WM CBF maps and a pseudo-CBF image was then created. In the second step, Gaussian PSF parameters were optimized to minimize the error between the CBF and resolution-adapted pseudo-CBF map. Afterwards, GM and WM CBF maps were updated using the estimated resolution and the two steps were iterated until convergence. Finally, weighted mean CBF_{1PLD}, CBF_{3PLD}, and CBF_{7PLD} values were extracted in left, right, and total cortex regions of interest (ROIs) using MATLAB (Mathworks, Natick, MA, USA, version R2023a), with partial volume values from the smoothed segmentations used as voxel-wise weights for the mean estimation.

2.5. Image quality assessment

The quality of structural scans (T1w and T2w) and the presence of fetal-type posterior cerebral artery variations were evaluated by a neuroradiologist with 8 years of experience (RDA), who was blinded to the rest of the dataset and clinical markers. Scans were categorized as "good" for excellent image quality or minor artifacts without significant degradation, "acceptable" for moderate artifacts visibly reducing image quality but not preventing diagnostic interpretation, and "unusable" for severe artifacts compromising diagnostic utility. The quality of ASL scans and the presence of artifacts were assessed by two researchers with 10+ and 4 years of ASL experience (JP and YP) based on the subtracted ASL images. To further ensure clinical relevance, all ASL scans were also reviewed by board-certified pediatric neuroradiologists (KWY and ET) as part of routine diagnostic workflow, and none were found to compromise or mislead diagnostic interpretation. Scans were classified as "good" if the perfusion signal was well-distributed in gray matter with no visible artifacts, "acceptable" if there were minor motion or macrovascular artifacts causing regional signal decrease but maintaining acceptable overall quality, and "unusable" if there were strong motion or macrovascular artifacts, or failed labeling rendering the scan non-diagnostic.

2.6. Statistical analysis

Statistical analyses and visualizations were performed using R (version 4.3.0). A sensitivity analysis of sex, PNA, GA, weight during scanning, birth weight, and causes of preterm birth among subdatasets of three ASL methods was performed using a chi-squared test and ANOVA. To assess the consistency of QC rating of within-session T1w and T2w scans, weighted Cohen's kappa with squared weights was calculated. To assess differences in scan quality distribution among ASL sequences, the Kruskal-Wallis test was used to account for the ordinality in classes. To assess the difference in the abundance of artifacts, a chi-squared test was used. A p-value$<$0.05 was considered statistically significant for all analyses.

ASL data marked as "unusable" were excluded from the consequent analysis of CBF and ATT distribution in preterm neonates. Paired t-tests with Satterthwaite correction for unequal variances and Cohen's d with Hedge's correction were applied to compare mean cortical CBF and ATT values among ASL variants and between sexes. To assess whether the difference between single- and multi-delay CBF values is associated with ATT variation, Pearson correlation analysis was performed between the differences in CBF_{3PLD} or CBF_{7PLD} and CBF_{1PLD}, and the corresponding ATT_{3PLD} or ATT_{7PLD} values, respectively.

Pearson correlation analysis was performed to assess the association of CBF and ATT with GA, PNA, and PMA. Age parameters with a significant correlation to hemodynamic parameters were then used in a linear regression model to predict cortical CBF or ATT.

CBF asymmetry between hemispheres was computed as:

$$Asymmetry = \frac{CBF_{left} - CBF_{right}}{CBF_{left}}$$

Positive values indicate higher CBF in the left cortex.

3. Results

3.1. Subject information

As shown in Fig. 1, forty-eight subjects were included in the analysis (25 males, mean GA 28.7 ± 2.6 weeks, mean PNA 9.7 ± 5.0 weeks, mean PMA 38.5 ± 3.4 weeks, mean weight at scanning 3.25 ± 1.20 kg, mean birth weight 1.13 ± 0.35). There was a significant correlation between GA and PNA age in the analyzed dataset ($r = -0.77$, $p < 0.001$). Overall, 10 (20.8%) participants were born due to spontaneous labor with intact membranes, 12 (25%) due to PPROM, 17 (35.4%) due to maternal indications, and 8 (16.7%) due to fetal indications. One participant (2.1%) had an unknown cause of birth, as the participant was transferred from another medical facility. All participants were scanned with $PCASL_{7PLD}$, 47 with $PCASL_{1PLD}$, and 37 with $PCASL_{3PLD}$; 36 subjects were scanned with all 3 sequences. Sensitivity analysis has not shown any significant differences in sex, PNA, GA, or weight at scanning among the subdatasets, as shown in Supplementary Table S2.

3.2. Image quality assessment

As shown in Table 1, quality control analysis of ASL data showed a significant difference both in scan quality and the abundance of artifacts among the sequences. $PCASL_{3PLD}$ sequence was least prone to artifacts and led to the best quality, while $PCASL_{7PLD}$ was the only sequence that suffered from an insufficient signal-to-noise ratio (SNR). $PCASL_{1PLD}$ was most prone to evident motion artifacts. The consistency of ASL scan quality among sequences is visualized in Fig. 2. Examples of quality assessment are shown in Supplementary Fig. S1.

Structural quality control showed much better quality for T2w scans (70.8% "good", 25% "acceptable", 4.2% "unusable") than for T1w scans (27% "good", 47.9% "acceptable", 25% "unusable"), with a fair agreement of within-session scores (kappa = 0.246, p = 0.0079). In the patients with "unusable" quality of T1w scans, the quality of ASL scans was below average (only

50% of $PCASL_{1PLD}$, 41.6% of $PCASL_{3PLD}$, and 66.6% of $PCASL_{7PLD}$ scans were of "good" or "acceptable" quality). Patients with "unusable" quality of T2w scans had 50% of $PCASL_{1PLD}$ and $PCASL_{7PLD}$ of "good" and "acceptable" quality.

3.3. CBF measurements

Cortical CBF_{1PLD} (mean 13.08 ± 4.28 ml/100 g/min) was significantly lower than cortical CBF_{3PLD} (mean 18.69 ± 5.56 ml/100 g/min, $p < 0.001$, $d = 1.12$), as well as cortical CBF_{7PLD} (mean 20.64 ± 6.06 ml/100 g/min, $p < 0.001$, $d = 1.43$), see Fig. 3. Cortical CBF_{1PLD} was significantly different between females (11.39 ± 4.14 ml/100 g/min) and males (14.37 ± 4.01 ml/100 g/min, $p = 0.035$, $d = 0.72$), but there was no significant difference between sexes in cortical CBF_{3PLD} nor in CBF_{7PLD} ($p = 0.16$, $d = 0.43$ and $p = 0.67$, $d = 0.14$, respectively), as shown in Supplementary Fig. S2. There was no significant difference between cortical CBF_{3PLD} and CBF_{7PLD} ($p = 0.16$, $d = 0.33$).

As shown in Fig. 4, Bland-Altman plots indicate the biggest difference in cortical CBF was observed between $PCASL_{1PLD}$ and $PCASL_{7PLD}$, also with the largest variance (mean bias 8.12 ml/100 g/min, 95% CI 5.85 – 10.40 ml/100 g/min, limits of agreement -4.14 – 20.39 ml/100 g/min). There was no significant correlation in the difference between CBF_{3PLD} and CBF_{1PLD} and ATT_{3PLD} ($r = -0.13$, $p = 0.51$), and no significant correlation in the difference between CBF_{7PLD} and CBF_{1PLD} and ATT_{7PLD} ($r = 0.35$, $p = 0.07$).

3.4. ATT distribution

As shown in Supplementary Fig. S2, group analysis of ATT showed no significant difference between ATT_{3PLD} (mean 1297.6 ± 160.8 ms) and ATT_{7PLD} (mean 1314.5 ± 308.6 ms, $p = 0.77$, Cohen's $d = 0.06$). There was a trend for longer ATT in males than females in both $PCASL_{3PLD}$ (male: 1331.8 ± 168.7 ms; female: 1238.4 ± 113.2 ms; $p = 0.0519$, $d = 0.61$) and $PCASL_{7PLD}$ (male: 1441.3 ± 418.3 ms; female: 1244.5 ± 165.1 ms; $p = 0.0453$, $d = 0.60$). There was no significant difference in ATT between subjects born prematurely due to fetal indications and subjects born due to other causes (ATT_{3PLD}: $p = 0.26$; $d = 0.54$; ATT_{7PLD}: $p = 0.14$, $d = 0.43$).

Table 1
Results of ASL quality control. The p-value indicates significance for the Kruskal-Wallis test (QC) and the chi-squared test (Artifacts).

		$PCASL_{7PLD}$	$PCASL_{3PLD}$	$PCASL_{1PLD}$	p-value
QC	Good	33 (68.8%)	31 (83.8%)	26 (55.3%)	0.0299
	Acceptable	5 (10.4%)	3 (8.1%)	11 (23.4%)	
	Unusable	10 (20.8%)	3 (8.1%)	10 (21.3%)	
Artifacts	No artifacts	33 (68.8%)	31 (83.8%)	26 (55.3%)	0.0076
	Lacking signal	3 (6.25%)	0	0	
	Motion	12 (25%)	6 (16.2%)	21 (44.7%)	

3.5. Relationship between hemodynamic values and age

As shown in Fig. 5, cortical CBF_{3PLD} and CBF_{1PLD} showed a significantly positive correlation with both PMA and PNA, while the relationship between CBF and age was insignificant for CBF_{7PLD}. Based on

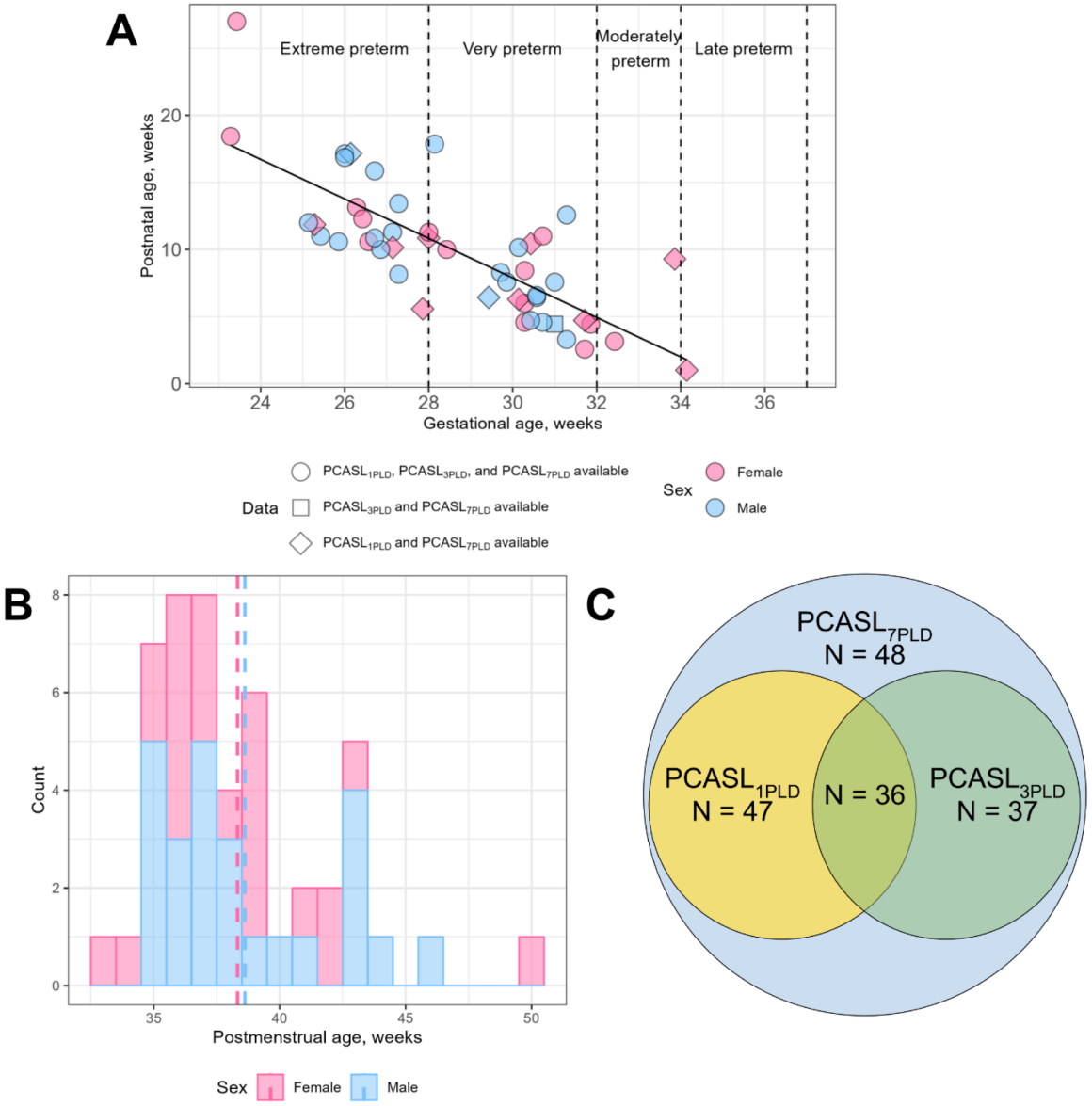

Fig. 1. Demographic characteristics of the analyzed dataset. **A.** Scatterplot showing the distribution of PNA and GA in the study population, along with data availability. **B.** Histogram illustrating the distribution of PMA in the analyzed population. Dashed lines indicate the mean PMA for female and male populations. **C.** Venn diagram representing the availability of data across sequence types.

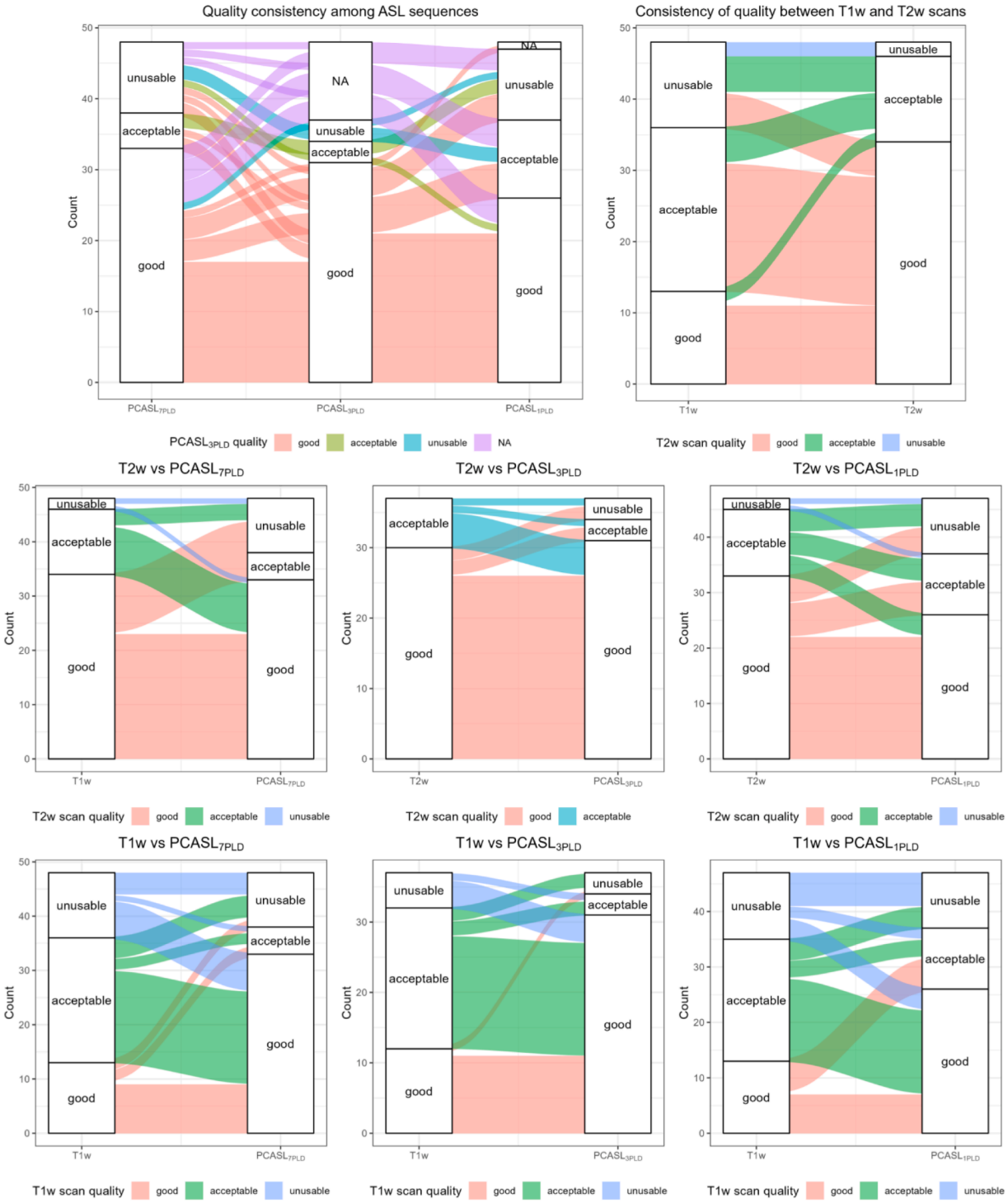

Fig. 2. Alluvial plot of quality consistency among ASL and structural sequences. Each vertical bar represents the distribution of scan quality (good, acceptable, unusable) for a given sequence. The colored lines (flows) connect the same individuals across different sequences and quality categories, visually representing how scan quality changes or remains consistent between sequences. The width of each line is proportional to the number of subjects with that specific quality transition. "NA" indicates scans that were not available.

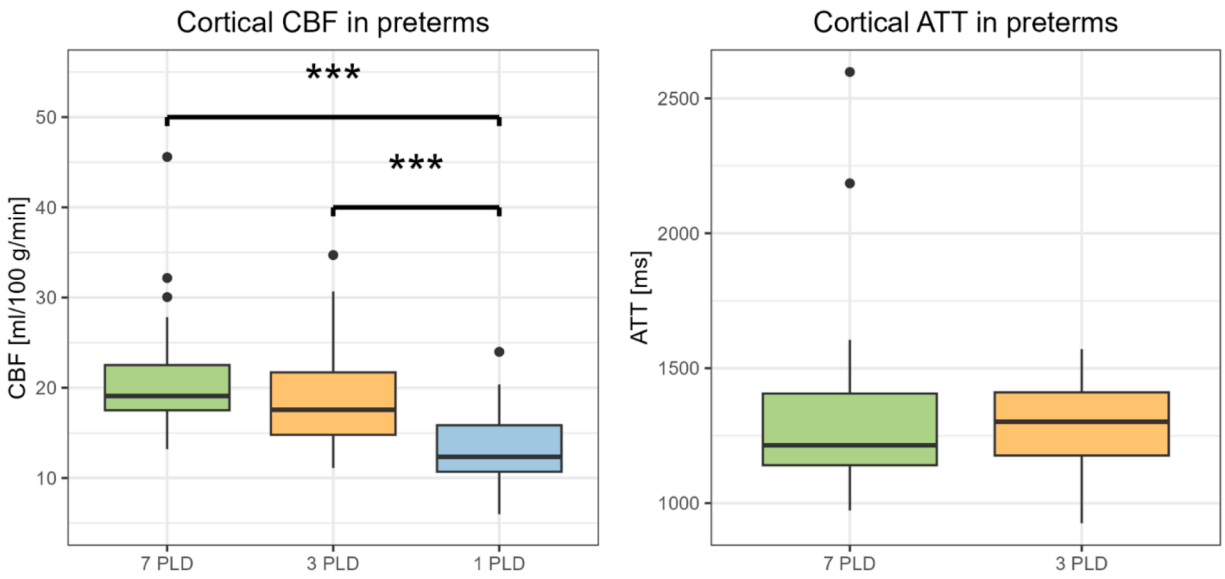

Fig. 3. Distribution of cortical CBF and ATT among acquisition methods. The central horizontal line represents the median, the box indicates the interquartile range, and the whiskers extend to the data points that lie within 1.5 × the interquartile range from the quartiles. Individual dots represent outliers beyond this range.

the correlation analysis, PNA and PMA were selected as predictors for linear regression modeling. Neither ATT_{3PLD} nor ATT_{7PLD} showed significant correlation with age (Supplementary Fig. S3). Participants prematurely born with fetal variants of the intracranial vasculature did not show a distinct trend in cortical CBF change with PNA (Supplementary Fig. S4).

In predicting CBF_{1PLD}, the linear regression model incorporating PNA explained a higher proportion of variance compared to the model using PMA (PNA: $R^2 = 17.7\%$, $p = 0.009$; PMA:

$R^2 = 13.5\%$, $p = 0.025$). Similarly, the model using PNA was more robust in predicting cortical CBF_{3PLD} than the model using PMA (PNA: $R^2 = 30.9\%$, $p < 0.001$; PMA: $R^2 = 28.4\%$, $p = 0.001$). However, neither PNA nor PMA emerged as statistically significant predictors for cortical CBF_{7PLD} (PNA: $p = 0.09$; PMA: $p = 0.06$).

3.6. CBF asymmetry

The distribution of relative CBF asymmetry is shown in Fig. 6. No significant variation from 0 in CBF asymmetry was observed ($PCASL_{1PLD}$ $p = 0.89$, $PCASL_{3PLD}$ $p = 0.40$, $PCASL_{7PLD}$ $p = 0.11$) with respect to PMA or fetal-type posterior cerebral artery variants. The distributions of relative CBF asymmetry remained consistent across all measurements: the mean relative asymmetry was -0.0018 ± 0.0755 for CBF_{1PLD}, 0.0107 ± 0.0742 for CBF_{3PLD}, and 0.0178 ± 0.0653 for CBF_{7PLD}.

4. Discussion

In this study, we compared hemodynamic values measured by single- and multi-delay ASL with matched acquisition times in a healthy preterm neonatal cohort. Our results show that multi-delay ASL sequences—particularly the three-delay protocol—achieved higher image quality and more consistent cortical CBF estimates compared to single-delay ASL. $PCASL_{3PLD}$ was shown to deliver the highest overall quality. Our CBF findings indicate that $PCASL_{1PLD}$ consistently yields lower cortical absolute CBF values compared to multi-delay acquisitions. CBF_{1PLD} and ATT_{7PLD} demonstrated significant differences in sex.

4.1. Neonatal MR imaging quality evaluation

Achieving high image quality remains a major challenge in many neonatal neuroimaging methods using MRI (Dubois et al., 2021). Our systematic assessment of scan quality demonstrated that $PCASL_{3PLD}$ achieved an optimal compromise between the number of repetitions and a limited range of post-labeling delays, yielding over 90% of scans rated as "good" or "acceptable" in quality. Although Hadamard-encoded ASL is generally expected to be more sensitive to motion artifacts compared to single- or sequential multi-PLD acquisitions (Woods et al., 2024), we observed a lower incidence of motion-affected scans in multi-delay ASL compared to ASL_{1PLD}. This may reflect not only physiological factors, such as unstable CBF and insufficient labeling delay in preterm neonates (Vesoulis & Mathur, 2017), but also the higher number of spiral arms in ASL_{1PLD}, which increases its sensitivity to motion. Although motion artifacts were less pronounced in $PCASL_{7PLD}$ compared to $PCASL_{1PLD}$, these scans were uniquely affected by signal deficiencies, suggesting a potential need for an increased number of repetitions to enhance signal robustness - an improvement that was observed in the $PCASL_{3PLD}$ protocol, which included more scans with longer PLD. Importantly, in addition to incorporating more scans with longer PLD, the $PCASL_{3PLD}$ protocol employed a substantially longer LD compared to $PCASL_{7PLD}$. This increased labeling duration likely contributed to the improved signal observed in $PCASL_{3PLD}$, underscoring the importance of LD as a key determinant of scan quality. As the overall acquisition quality depends on the exact scanning procedure, we have compared the quality of the structural scans with prior findings. Our findings exhibited increased overall quality (95% of T2w scans and 74% of T1w scans rated as "good" or "acceptable) compared to earlier studies reporting motion artifacts in 56% of MPRAGE and 50% of T2 TSE scans in non-sedated neonates (Hughes et al., 2017). Importantly, ASL scans were often interpretable even when T1w and T2w images were rated as unusable, supporting the complementary role of perfusion imaging when structural quality is limited. To further ensure clinical relevance, all ASL scans were reviewed by board-certified pediatric neuroradiologists as part of routine diagnostic workflow, and none were found to compromise or mislead diagnostic interpretation.

4.2. Comparing neonatal hemodynamic values across ASL techniques

A key contribution of our study is systematically comparing CBF values obtained from single- and multi-delay ASL within a single scanning session in preterm neonates. Significant differences were observed between CBF_{1PLD} and multi-delay CBF. While CBF_{1PLD} aligns with previously reported GM CBF values in similar populations, multi-delay CBF

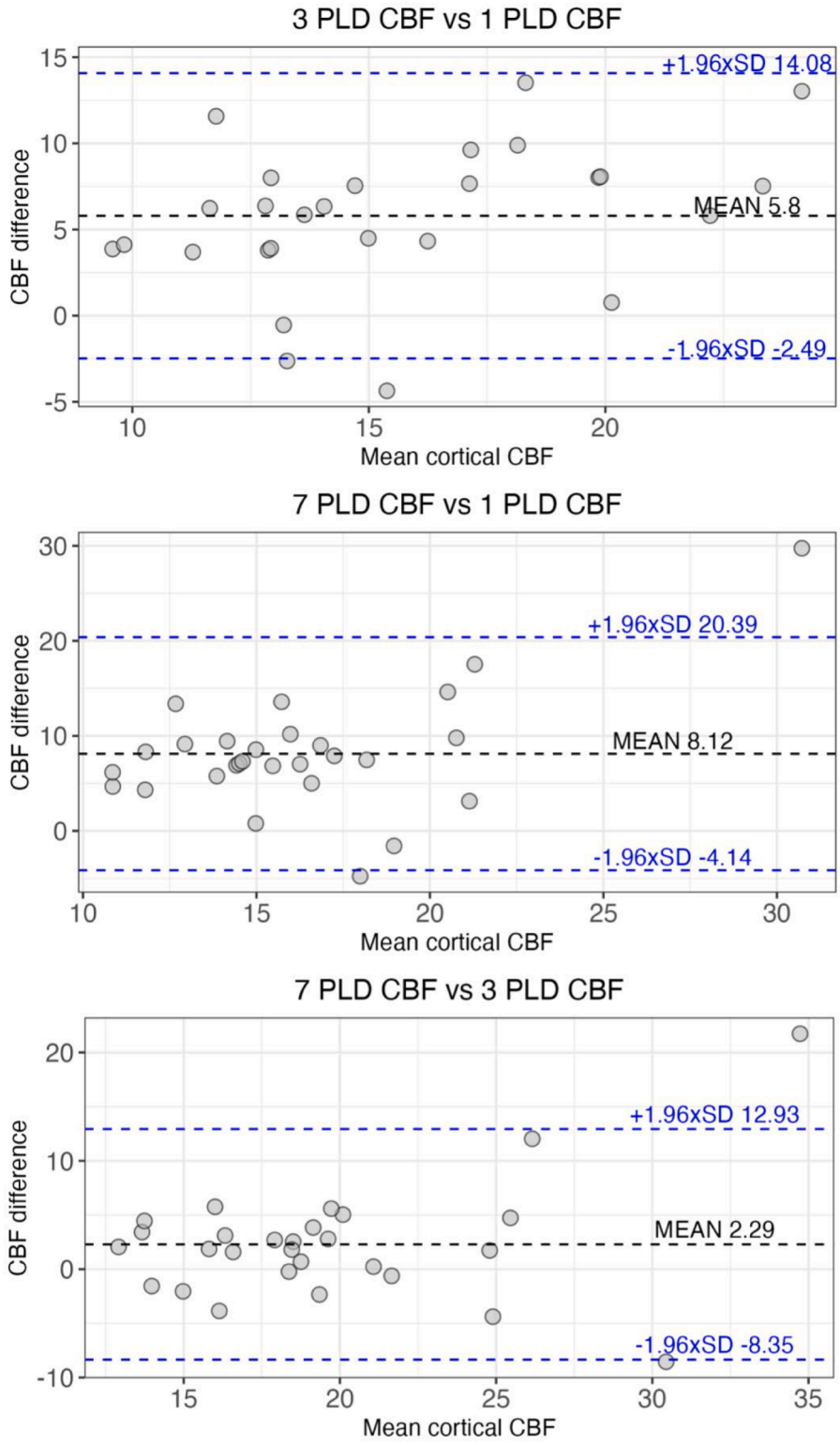

Fig. 4. Bland-Altman plots of cortical CBF agreement among methods. "Mean" indicates mean bias, and "±1.96xSD" indicate limits of agreement.

values are consistent with those obtained from sonographic flowmetry, Xe-133 imaging, NIRS (Leon et al., 2022, Proisy et al., 2016), and another multi-delay ASL study (Kim et al., 2022). Discrepancies between single- and multi-delay CBF have also been noted in full-term newborns (Hu et al., 2025), though differences in multi-delay values may reflect the impact of advanced large-vessel signal suppression techniques, which may be due to large-vessel signal artifacts. Comparing neonatal ASL techniques with and without vascular artifacts suppression may be pursued in future studies.

The divergence between single- and multi-delay CBF in preterm neonates likely stems from slower blood flow and impaired cerebral autoregulation, leading to regional CBF variability. This variability, most pronounced in the early postnatal period, may persist for months, contributing to long-term neurodevelopmental deficits (Kooi et al.,

2017) and is particularly relevant in neonates at elevated risk of brain injury (Pfurtscheller et al., 2023). Variability in CBF can also be linked with ATT variability, reducing SNR in $PCASL_{1PLD}$, which may not be adequately compensated by increased repetitions. This issue is exacerbated by ATT values, which are higher in neonates than in adult populations, consistent with previous studies (Hu et al., 2025, Kim et al., 2022). This limitation may reduce the clinical utility of $PCASL_{1PLD}$ in at-risk preterm neonates, suggesting the potential benefit of incorporating longer PLDs in this population.

4.3. *Impact on neonatal hemodynamics due to sex, age, and vascular anatomical variations*

Our results indicate that ATT may be longer in males compared to females (ATT_{7PLD} p = 0.0453, ATT_{3PLD} p = 0.0519), suggesting sex-related differences in blood arrival times, which may influence CBF quantification. These findings align with previous Doppler ultrasound studies in full-term infants following chorioamnionitis, which reported sex-related differences in blood velocities and vessel resistance (Koch et al., 2014). highlighting complex, sex-specific hemodynamic variations in neonates. In addition to ATT differences, significant sex-related differences in CBF_{1PLD} were also observed in this study. However, prior research on sex-related CBF differences has been inconsistent: while

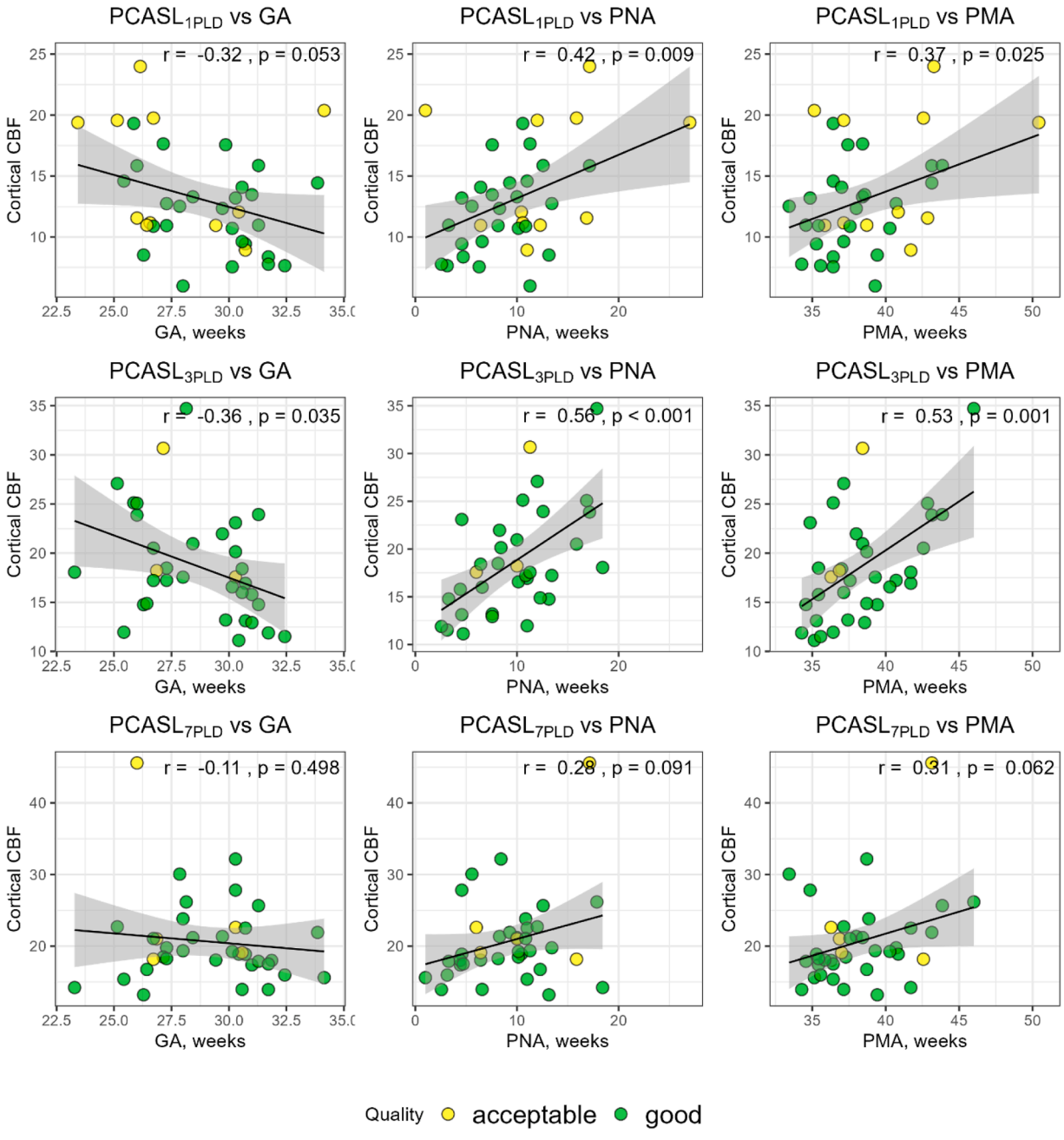

Fig. 5. Correlation between cortical CBF parameters and GA, PNA, PMA. "r" represents the Pearson correlation coefficient, and "p" indicates the corresponding p-value from the relevant correlation test. The gray shaded area represents the standard error of the estimated correlation.

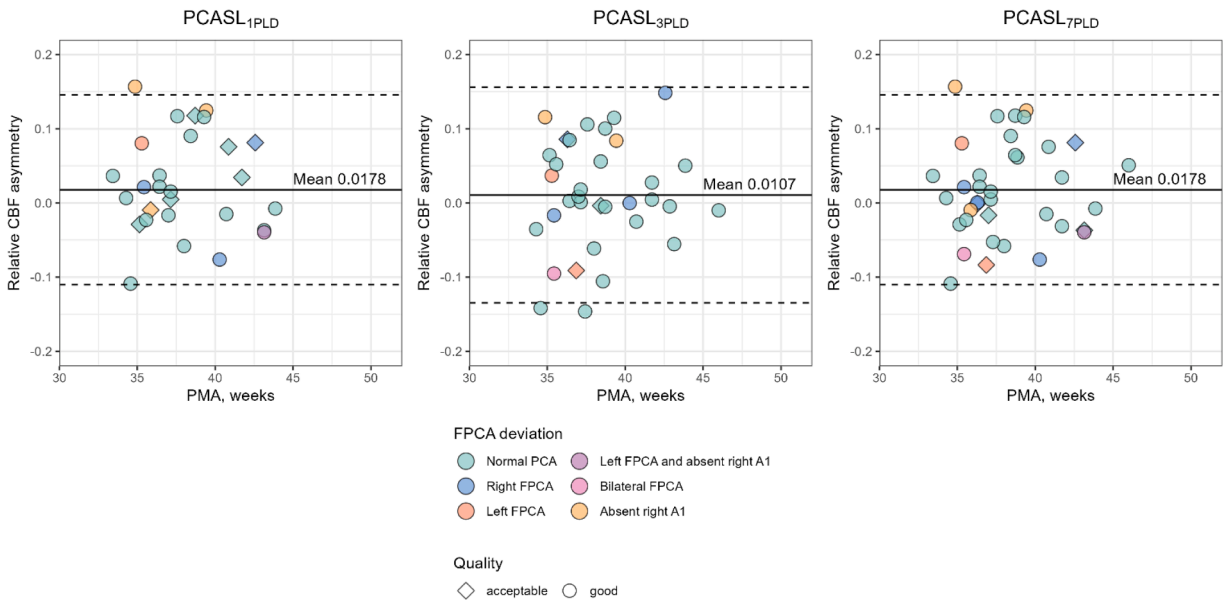

Fig. 6. Relative hemispheric CBF asymmetry observed in neonates. *FPCA* - fetal-type posterior cerebral artery.

higher CBF in males has been reported using NIRS and Xenon-133 imaging, consistent with our findings (Baenziger et al., 1994, Lin et al., 2013). lower CBF in males has been observed with single-delay pseudo-continuous ASL (Wang et al., 2019) and pulsed ASL (Zheng et al., 2021). These discrepancies may be attributed to quantification bias related to differences in ATT, with males typically exhibiting prolonged ATT. This difference is particularly relevant in studies using single-delay ASL techniques, which are more sensitive to variations in arrival time. These results underscore the advantages of using multi-delay ASL to account for such variability and accurately characterize cerebral perfusion. The established male disadvantage in neonatal brain injury and encephalopathy outcomes (Kelly et al., 2023) further emphasizes the importance of investigating sex-related differences in CBF and ATT to better understand underlying mechanisms and guide clinical interventions.

Positive correlations between both cortical CBF_{1PLD} and CBF_{3PLD} and both PNA and PMA were found, consistent with prior studies (Zun et al., 2021, Benders et al., 2011, Meng et al., 2021). Only CBF_{3PLD} showed a significant negative correlation with GA, supporting earlier findings of higher CBF in preterm compared to full-term neonates (Tortora et al., 2017). However, as reported in a seven-delay ASL study, no significant correlation with GA was observed (Kim et al., 2022). The lack of correlation between CBF_{7PLD}, as well as ATT parameters and age may reflect the complex interplay between perfusion and neurovascular development during the early postnatal adaptation period.

Our results on CBF differences due to cerebral vascular variations showed no significant contralateral asymmetries, despite previous reports of right hemisphere metabolic dominance in smaller newborns (Lin et al., 2013). Fetal-type posterior cerebral artery variants exhibited an ambiguous influence on cerebral perfusion laterality. Future studies investigating perfusion changes across vascular territories are recommended to better understand the impact of fetal-type PCA variants on early-life hemodynamics.

4.4. Clinical implications

The findings of our study have direct clinical relevance for the evolving role of ASL in neonatal brain imaging. As preterm neonates often undergo MRI for early detection of brain injury and prognostic evaluation, incorporating multi-delay ASL protocols would offer more accurate and interpretable hemodynamic outcomes. Improved sensitivity to ATT and reduced susceptibility to motion artifacts, particularly in $PCASL_{3PLD}$, may allow clinicians to assess cerebral hemodynamics even when structural sequences are degraded. This is crucial for non-sedated, medically fragile neonates where imaging time is constrained. Moreover, as CBF patterns increasingly inform risk stratification, neuroprotective interventions, and follow-up planning, standardizing delay-sensitive ASL protocols across institutions could help translate advanced imaging techniques into actionable clinical insights. Future studies may focus on validating standardized multi-delay ASL protocols across centers.

In clinical practice, distinguishing between technical factors, such as motion artifacts or poor labeling efficiency, and true hypoperfusion is a critical challenge in interpreting neonatal ASL images, as both can produce similarly low CBF signals. To improve diagnostic confidence, it is recommended that ASL CBF maps are assessed alongside structural MRI images to provide anatomical context and help identify regions where low perfusion may correspond to injury or artifact. Reviewing the raw perfusion-weighted images of individual PLDs for outliers or scans with pronounced artifacts can also be valuable, as these may skew CBF values. Assessing the homogeneity of CBF spatial distribution can help detect technical failures; for example, missing signal in a specific vascular territory or hemisphere may suggest failed labeling, while halo effects around the brain are often indicative of motion. However, reliably distinguishing true pathology from technical artifacts remains challenging, particularly for neuroradiologists without specialized ASL training. Incorporating standard quality control steps and providing dedicated ASL training may help increase the reliability and broader clinical utility of ASL in preterm neonates.

4.5. Limitations

This study has several limitations. First, the single-delay ASL protocol employed a short post-labeling delay (PLD) of 1525 ms. Although the ASL consensus white paper recommends a PLD 2000 ms for neonates (Alsop et al., 2015), we used a shorter PLD as it is the default setting in our single-PLD ASL sequence, which was not optimized specifically for this population. Using a longer PLD could improve the signal-to-noise ratio and reduce discrepancies between single- and multi-delay CBF measurements. Although T2w images had better scan quality, ASL scans

were registered to T1w scans despite their susceptibility to artifacts. However, the 2D acquisition and thicker slices of T2w scans can introduce partial volume effects, potentially reducing registration precision. While large-vessel signal can inflate regional CBF values (Hu et al., 2025), we excluded deep GM regions to minimize this artifact, focusing instead on cortical perfusion. In neonates, ASL is particularly susceptible to macrovascular contamination due to slower flow velocities and prolonged ATT, which can cause labeled spins to dwell in large vessels and generate spurious hyperintensities, even at long post-labeling delays. In addition, different acquisition parameters were used for $PCASL_{1PLD}$, $PCASL_{3PLD}$, and $PCASL_{7PLD}$ sequences. We addressed practical differences in effective resolution by applying appropriate smoothing to the segmentation maps, aiming to reflect typical clinical scenarios using default scanner settings. Future work may focus more specifically on optimizing acquisition parameters for improved ASL performance in preterm neonates. The aim of this study was to evaluate the quality of neonatal neuroimaging rather than the performance of the raters; therefore, inter-rater agreement was not assessed. However, further studies evaluating inter-rater variability are recommended to better understand the stability of clinical ASL image evaluation in neonates. Neonatal blood T1 values are higher and more variable than in adults due to lower hematocrit levels in early life (Varela et al., 2011). Ideally, CBF quantification should incorporate individual hematocrit or blood T1 measurements. In this study, however, scanner-reconstructed ASL images were processed using a fixed blood T1 value for both single- and multi-PLD protocols, which may have introduced bias in the absolute CBF estimates. Nevertheless, since both ASL sequences were acquired within the same session, intra-subject hematocrit variation is unlikely to have affected within-subject comparisons. Furthermore, sensitivity analyses showed no significant differences in GA, PNA, sex, or birth weight across subgroups – factors potentially impacting hematocrit (Jopling et al., 2009) – suggesting minimal inter-group hematocrit variability. We recommend that future studies systematically collect hematocrit data to support individualized quantification and improve the accuracy and standardization of ASL in neonatal populations. Excluding outlier scans with pronounced artifacts and manually quantifying CBF and ATT maps could further improve perfusion image quality. While these approaches require additional processing time and expertise and are not routinely available in standard clinical-scanner software, they may be especially beneficial in populations prone to motion or other artifacts. Nonetheless, scanner-reconstructed CBF and ATT maps were used in this study to assess the clinical applicability of ASL with minimal post-processing, in line with current clinical practice. Finally, the limited sample size may have constrained the statistical power of certain analyses, such as age correlations for ASL_{7PLD} and sex-related differences, where positive correlation coefficients and large effect sizes suggest potential trends warranting further investigation. Larger cohort studies are recommended to comprehensively analyze the impact of causes of preterm birth on hemodynamic changes and the influence of structural variants of posterior cerebral artery on perfusion asymmetries in a neonatal brain.

As the field of ASL in neonates remains in early stages, there is a wide range of unresolved methodological and clinical questions. We intentionally explored multiple acquisition strategies and analytical approaches to address key variables—such as ATT, labeling parameters, age effects, and image quality—that influence clinical utility. While some analyses may be exploratory in nature, this broader approach reflects the current need for foundational data in this population. We hope that these findings will guide both clinical application and the design of future targeted investigations.

5. Conclusions

A key contribution of our study is the systematic evaluation of scan quality and artifact prevalence across three ASL acquisition techniques matched for acquisition time, offering a foundation for their clinical implementation in preterm neonates. Our findings demonstrate that a three-delay ASL protocol provides an optimal compromise between the limited number of PLDs and scan repetitions, while T2w scans exhibited superior image quality compared to T1w. Motion artifacts, a prominent challenge in neonatal imaging, were less pronounced in Hadamard-encoded ASL compared to single-delay ASL, highlighting its potential robustness for this population. We found that single-delay ASL consistently yielded lower cortical CBF values compared to multi-delay ASL. Furthermore, significant sex-based differences in CBF and ATT were identified, underscoring the importance of accounting for these variations, particularly in studies utilizing single-delay ASL.

Funding

This study was supported by the Czech Health Research Council (project no. NU23-08-00460), the project no. LX22NPO5107 (MEYS), financed by the European Union – Next Generation EU, the Stanford Maternal and Child Health Research Institute Team Science and Translational Medicine Faculty Development Program, and the American Heart Association (grant no. 23SCEFIA1141920). JP received funding from the European Union's Horizon Europe WIDERA program under grant agreement no. 101159624 (TACTIX). YP was awarded the ISMRM Research Exchange Program Grant.

Data and code availability statement

The datasets used in this study are not publicly available; however, requests for access may be made upon reasonable request to the Corresponding Author.

CRediT authorship contribution statement

Yeva Prysiazhniuk: Writing – review & editing, Writing – original draft, Methodology, Investigation, Formal analysis, Conceptualization. **Sasha Alexander:** Validation, Project administration, Data curation. **Rui Duarte Armindo:** Methodology, Investigation, Conceptualization. **Elizabeth Tong:** Methodology, Data curation. **Kristen W Yeom:** Methodology, Data curation. **Jakub Otáhal:** Writing – review & editing. **Martin Kynčl:** Writing – review & editing. **Michael Moseley:** Writing – review & editing, Supervision. **Jan Petr:** Software, Methodology, Investigation. **Moss Y Zhao:** Writing – review & editing, Supervision, Funding acquisition, Conceptualization. **Gary K Steinberg:** Writing – review & editing, Supervision.

Declaration of competing interest

The authors have no personal, financial, or institutional interest in any of the drugs, materials, or devices described in this article. Dr. Steinberg is a consultant for SanBio, Zeiss, Peter Lazic US, Surgical Theater, and Recursion Therapeutics.

Supplementary materials

Supplementary material associated with this article can be found, in the online version, at doi:10.1016/j.neuroimage.2025.121511.

References

Alsop, D.C., Detre, J.A., Golay, X., Günther, M., Hendrikse, J., Hernandez-Garcia, L., et al., 2015. Recommended implementation of arterial spin-labeled perfusion MRI for clinical applications: A consensus of the ISMRM perfusion study group and the European consortium for ASL in dementia. Magn. Reson. Med. 73 (1), 102–116.

Andersen, J.B., Lindberg, U., Olesen, O.V., Benoit, D., Ladefoged, C.N., Larsson, H.B., et al., 2019. Hybrid PET/MRI imaging in healthy unsedated newborn infants with quantitative rCBF measurements using 15O-water PET. J. Cereb. Blood Flow Metab. 39 (5), 782–793. May 1.

Baenziger, O., Jaggi, J.L., Mueller, A.C., Morales, C.G., Lipp, H.P., Lipp, A.E., et al., 1994. Cerebral blood flow in preterm infants affected by sex, mechanical ventilation, and intrauterine growth. Pediatr. Neurol. 11 (4), 319–324. Nov 1.

Benders, M., Hendrikse, J., de Vries, L.S., van Bel, F., Groenendaal, F., 2011. Phase-contrast magnetic resonance angiography measurements of global cerebral blood flow in the neonate. Pediatr. Res. 69 (6), 544–547. Jun.

Bouyssi-Kobar, M., Murnick, J., Brossard-Racine, M., Chang, T., Mahdi, E., Jacobs, M., et al., 2018. Altered cerebral perfusion in infants born preterm compared with infants born full term. J. Pediatr. 193, 54–61.e2. Feb.

Davis, A.S., Hintz, S.R., Goldstein, R.F., Ambalavanan, N., Bann, C.M., Stoll, B.J., et al., 2014. Outcomes of extremely preterm infants following severe intracranial hemorrhage. J. Perinatol. Off J. Calif. Perinat. Assoc. 34 (3), 203–208. Mar.

Dubois, J., Alison, M., Counsell, S.J., Hertz-Pannier, L., Hüppi, P.S., Benders, M., 2021. MRI of the neonatal brain: a review of methodological challenges and neuroscientific advances. J. Magn. Reson. Imaging. 53 (5), 1318–1343.

Dubois, M., Legouhy, A., Corouge, I., Commowick, O., Morel, B., Pladys, P., et al., 2021. Multiparametric analysis of cerebral development in preterm infants using magnetic resonance imaging. Front. Neurosci. 15, 658002.

Fukuda, S., Mizuno, K., Kakita, H., Kato, T., Hussein, M.H., Ito, T., et al., 2008. Late circulatory dysfunction and decreased cerebral blood flow volume in infants with periventricular leukomalacia. Brain Dev. 30 (9), 589–594. Oct 1.

Goldenberg, R.L., Culhane, J.F., Iams, J.D., Romero, R., 2008. Epidemiology and causes of preterm birth. Lancet 371 (9606), 75–84. Jan 5.

Hak, J.F., Boulouis, G., Kerleroux, B., Benichi, S., Stricker, S., Gariel, F., et al., 2022. Arterial Spin labeling for the etiological workup of intracerebral hemorrhage in children. Stroke 53 (1), 185–193. Jan.

Hendrickson, T.J., Reiners, P., Moore, L.A., Lundquist, J.T., Fayzullobekova, B., Perrone, A.J., et al., 2025. BIBSNet: a deep learning baby image brain segmentation network for MRI scans. bioRxiv. Jan 112023.03.22.533696.

Hu, Z., Jiang, D., Shepard, J., Uchida, Y., Oishi, K., Shi, W., et al., 2025. High-fidelity MRI assessment of cerebral perfusion in healthy neonates less than 1 week of age. J. Magn. Reson. Imaging 62 (3), 737–748. https://doi.org/10.1002/jmri.29740.

Hughes, E.J., Winchman, T., Padormo, F., Teixeira, R., Wurie, J., Sharma, M., et al., 2017. A dedicated neonatal brain imaging system. Magn. Reson. Med. 78 (2), 794–804.

Jopling, J., Henry, E., Wiedmeier, S.E., Christensen, RD., 2009. Reference ranges for hematocrit and blood hemoglobin concentration during the neonatal period: data from a multihospital health care system. Pediatrics 123 (2), e333–e337. Feb 1.

Kelly, L.A., Branagan, A., Semova, G., Molloy, EJ., 2023. Sex differences in neonatal brain injury and inflammation. Front. Immunol. 14, 1243364.

Kim, H.G., Choi, J.W., Lee, J.H., Jung, D.E., Gho, SM., 2022. Association of cerebral blood flow and brain tissue relaxation time with neurodevelopmental outcomes of preterm neonates: multidelay arterial spin labeling and synthetic MRI Study. Invest. Radiol. 57 (4), 254. Apr.

Kleiser, S., Nasseri, N., Andresen, B., Greisen, G., Wolf, M., 2016. Comparison of tissue oximeters on a liquid phantom with adjustable optical properties. Biomed. Opt. Express. 7 (8), 2973–2992. Jul 11.

Koch, F.R., Wagner, C.L., Jenkins, D.D., Caplan, M.J., Perkel, J.K., Rollins, L.G., et al., 2014. Sex differences in cerebral blood flow following chorioamnionitis in healthy term infants. J. Perinatol. 34 (3), 197–202. Mar.

Kooi, E.M.W., Verhagen, E.A., Elting, J.W.J., Czosnyka, M., Austin, T., Wong, F.Y., et al., 2017. Measuring cerebrovascular autoregulation in preterm infants using near-infrared spectroscopy: an overview of the literature. Expert. Rev. NeurOther. 17 (8), 801–818. Aug 3.

Langley, E.A., Blake, S.M., Coe, KL., 2022. Recent review of germinal matrix hemorrhage-intraventricular hemorrhage in preterm infants. Neonatal Netw. NN 41 (2), 100–106. Mar 1.

Leon, R.L., Ortigoza, E.B., Ali, N., Angelis, D., Wolovits, J.S., Chalak, LF., 2022. Cerebral blood flow monitoring in high-risk fetal and neonatal populations. Front. Pediatr. 9, 748345. Jan 11.

Lin, P.Y., Roche-Labarbe, N., Dehaes, M., Fenoglio, A., Grant, P.E., Franceschini, MA., 2013. Regional and hemispheric asymmetries of cerebral hemodynamic and oxygen metabolism in newborns. Cereb. Cortex N. Y. N 1991 23 (2), 339–348. Feb.

Meng, L., Wang, Q., Li, Y., Ma, X., Li, W., Wang, Q., 2021. Diagnostic performance of arterial spin-labeled perfusion imaging and diffusion-weighted imaging in full-term neonatal hypoxic-ischemic encephalopathy. J. Integr. Neurosci. 20 (4), 985–991. Dec 30.

Mutsaerts, H., Petr, J., Groot, P., Vandemaele, P., Ingala, S., Robertson, A.D., et al., 2020. ExploreASL: An image processing pipeline for multi-center ASL perfusion MRI studies. Neuroimage 219, 117031. Oct 1.

Ohuma, E.O., Moller, A.B., Bradley, E., Chakwera, S., Hussain-Alkhateeb, L., Lewin, A., et al., 2023. National, regional, and global estimates of preterm birth in 2020, with trends from 2010: a systematic analysis. Lancet 402 (10409), 1261–1271. Oct 7.

Pfurtscheller, D., Baik-Schneditz, N., Schwaberger, B., Urlesberger, B., Pichler, G., 2023. Insights into neonatal cerebral autoregulation by blood pressure monitoring and cerebral tissue oxygenation: a qualitative systematic review. Children 10 (8), 1304. Aug.

Proisy, M., Mitra, S., Uria-Avellana, C., Sokolska, M., Robertson, N.J., Jeune, F.L., et al., 2016. Brain perfusion imaging in neonates: an overview. Am. J. Neuroradiol. 37 (10), 1766–1773. Oct 1.

Sarda, S.P., Sarri, G., Siffel, C., 2021. Global prevalence of long-term neurodevelopmental impairment following extremely preterm birth: a systematic literature review. J. Int. Med. Res. 49 (7), 03000605211028026. Jul 1.

Singh, Y., Villaescusa, J.U., da Cruz, E.M., Tibby, S.M., Bottari, G., Saxena, R., et al., 2020. Recommendations for hemodynamic monitoring for critically ill children—expert consensus statement issued by the cardiovascular dynamics section of the European Society of Paediatric and Neonatal Intensive Care (ESPNIC). Crit. Care 24 (1), 620. Oct 22.

Tortora, D., Mattei, P.A., Navarra, R., Panara, V., Salomone, R., Rossi, A., et al., 2017. Prematurity and brain perfusion: arterial spin labeling MRI. Neuroimage Clin. 15, 401–407. May 26.

Tuura, R.O., Kottke, R., Brotschi, B., Sabandal, C., Hagmann, C., Latal, B., 2024. Elevated cerebral perfusion in neonatal encephalopathy is associated with neurodevelopmental impairments. Pediatr. Res. 1–8. Sep 17.

Varela, M., Hajnal, J.V., Petersen, E.T., Golay, X., Merchant, N., Larkman, DJ., 2011. A method for rapid in vivo measurement of blood T1. NMR Biomed. 24 (1), 80–88. Jan.

Vesoulis, Z.A., Mathur, AM., 2017. Cerebral Autoregulation, brain injury, and the transitioning premature infant. Front. Pediatr. 5, 64. https://doi.org/10.3389/fped.2017.00064. Published 2017 April 3.

Wang, J.N., Li, J., Liu, H.J., Yin, X.P., Zhou, H., Zheng, Y.T., et al., 2019. Application value of three-dimensional arterial spin labeling perfusion imaging in investigating cerebral blood flow dynamics in normal full-term neonates. BMC. Pediatr. 19 (1), 495. Dec 13.

Woods, J.G., Achten, E., Asllani, I., Bolar, D.S., Dai, W., Detre, J.A., et al., 2024. Recommendations for quantitative cerebral perfusion MRI using multi-timepoint arterial spin labeling: Acquisition, quantification, and clinical applications. Magn. Reson. Med. 92 (2), 469–495.

Younkin, D., Delivoria-Papadopoulos, M., Reivich, M., Jaggi, J., Obrist, W., 1988. Regional variations in human newborn cerebral blood flow. J. Pediatr. 112 (1), 104–108. Jan.

Younkin, D.P., Reivich, M., Jaggi, J.L., Obrist, W.D., 1987. Delivoria-Papadopoulos M. The effect of hematocrit and systolic blood pressure on cerebral blood flow in newborn infants. J. Cereb. Blood Flow Metab. Off. J. Int. Soc. Cereb. Blood Flow Metab. 7 (3), 295–299. Jun.

Zamora, C., Tekes, A., Alqahtani, E., Kalayci, O.T., Northington, F., Huisman, Ta.GM., 2014. Variability of resistive indices in the anterior cerebral artery during fontanel compression in preterm and term neonates measured by transcranial duplex sonography. J. Perinatol. Off. J. Calif. Perinat. Assoc. 34 (4), 306–310. Apr.

Zheng, Q., Freeman, C.W., Hwang, M., 2021. Sex-related differences in arterial spin-labelled perfusion of metabolically active brain structures in neonatal hypoxic–ischaemic encephalopathy. Clin. Radiol. 76 (5), 342–347. May 1.

Zun, Z., Kapse, K., Jacobs, M., Basu, S., Said, M., Andersen, N., et al., 2021. Longitudinal trajectories of regional cerebral blood flow in very preterm infants during third trimester ex utero development assessed with MRI. Radiology 299 (3), 691–702. Jun.